



Measurement of the doubly-polarized ${}^3\text{He}(\vec{\gamma}, n)pp$ reaction at 16.5 MeV and its implications for the GDH sum rule



G. Laskaris^{a,b,*}, X. Yan^{a,b}, J.M. Mueller^{a,b,1}, W.R. Zimmerman^{a,b}, W. Xiong^{a,b}, M.W. Ahmed^{a,b,c}, T. Averett^d, P.-H. Chu^{a,b,2}, A. Deltuva^e, C. Flower^{a,b}, A.C. Fonseca^f, H. Gao^{a,b}, J. Golak^g, J.N. Heideman^{a,h}, H.J. Karwowski^{a,h}, M. Mezziane^{a,b}, P.U. Sauerⁱ, R. Skibiński^g, I.I. Strakovsky^j, H.R. Weller^{a,b}, H. Witała^g, Y.K. Wu^{a,b}

^a Triangle Universities Nuclear Laboratory, Durham, NC 27708, USA

^b Department of Physics, Duke University, Durham, NC 27708, USA

^c Department of Mathematics and Physics, North Carolina Central University, Durham, NC 27707, USA

^d College of William and Mary, Williamsburg, VA 23187, USA

^e Institute of Theoretical Physics and Astronomy, Vilnius University, LT-01108 Vilnius, Lithuania

^f Centro de Física Nuclear da Universidade de Lisboa, P-1649-003 Lisboa, Portugal

^g M. Smoluchowski Institute of Physics, Jagiellonian University, PL-30348 Kraków, Poland

^h Department of Physics and Astronomy, University of North Carolina at Chapel Hill, Chapel Hill, NC 27599, USA

ⁱ Institut für Theoretische Physik, Leibniz Universität Hannover, D-30167 Hannover, Germany

^j Department of Physics, The George Washington University, Washington, DC 20052, USA

ARTICLE INFO

Article history:

Received 23 July 2015

Received in revised form 23 September 2015

Accepted 28 September 2015

Available online 1 October 2015

Editor: D.F. Geesaman

Keywords:

GDH sum rule

Polarized ${}^3\text{He}$

Photoabsorption

Polarization observables

ABSTRACT

We report new measurements of the double-polarized photodisintegration of ${}^3\text{He}$ at an incident photon energy of 16.5 MeV, carried out at the High Intensity γ -ray Source (HI γ S) facility located at Triangle Universities Nuclear Laboratory (TUNL). The spin-dependent double-differential cross sections and the contribution from the three-body channel to the Gerasimov–Drell–Hearn (GDH) integrand were extracted and compared with the state-of-the-art three-body calculations. The calculations, which include the Coulomb interaction and are in good agreement with the results of previous measurements at 12.8 and 14.7 MeV, deviate from the new cross section results at 16.5 MeV. The GDH integrand was found to be about one standard deviation larger than the maximum value predicted by the theories.

© 2015 The Authors. Published by Elsevier B.V. This is an open access article under the CC BY license (<http://creativecommons.org/licenses/by/4.0/>). Funded by SCOAP³.

1. Introduction

An important window for the study of QCD is through the investigation of the structure and particularly the spin structure of the nucleon and few-body nuclei. Therefore sum rules involving the spin structure of the nucleon or nuclei are nowadays at the forefront of intensive experimental and theoretical efforts. Among spin sum rules, the GDH sum rule [1] is particularly interesting. This sum rule relates the energy-weighted difference of the spin-

dependent total photo-absorption cross sections σ^P (σ^A) for target spin and beam helicity parallel (antiparallel) to static properties of the target nucleon/nucleus, i.e. the anomalous magnetic moment and the mass, as follows:

$$I^{GDH} = \int_{\nu_{thr}}^{\infty} (\sigma^P - \sigma^A) \frac{d\nu}{\nu} = \frac{4\pi^2\alpha}{M^2} \kappa^2 I, \quad (1)$$

where ν is the photon energy, ν_{thr} is the pion production/photodisintegration threshold on the nucleon/nucleus, α is the fine structure constant, κ is the anomalous magnetic moment, M is the mass and I is the spin of the nucleon/nucleus. There have been worldwide efforts in testing the GDH sum rule on proton and neutron [2,3]. More recently, experimental investigations of the GDH

* Corresponding author. Currently at Stanford University, Stanford, CA 94305, USA.

E-mail address: laskaris@stanford.edu (G. Laskaris).

¹ Currently at NCSU, Raleigh, NC 27695, USA.

² Currently at LANL, Los Alamos, NM 87544, USA.

sum rule on nuclei such as the deuteron [4–6] and ^3He [7–10] have begun.

The determination of the GDH sum rule on ^3He at the energy region between the two-body photodisintegration (~ 5.5 MeV) and pion production thresholds (~ 140 MeV) is particularly interesting for a number of reasons. This energy region has an important contribution to the overall sum rule [8,11] and it is a region where one can test state-of-the-art three-body calculations. The experimental determination of the GDH integral on ^3He can also test to what extent a polarized ^3He target is an effective polarized neutron target. A polarized ^3He target is commonly used as a polarized neutron target to extract the electromagnetic form factors [12–14] and the spin structure functions [15,16] of the neutron since the nuclear spin of ^3He is carried mostly by the unpaired neutron. To acquire information about the neutron using a polarized ^3He target, nuclear corrections relying on three-body calculations need to be used, but first they must be validated by experiments.

The GDH integral below pion threshold can be estimated based on three-body calculations which are performed mainly through the machinery of Faddeev [17] and Alt–Grassberger–Sandhas equations (AGS) [18] and have been carried out for both two-body and three-body photodisintegration of ^3He with double polarization. These calculations [19,20] use a variety of nucleon–nucleon (NN) potentials like Argonne V18 (AV18) [21] or CD Bonn [22,23] and three-nucleon forces (3NFs) like Urbana IX (UIX) [24] or CD Bonn + Δ [19], with the latter yielding an effective 3NF through the Δ -isobar excitation. The plateau value that both sets of calculations [19,20] predict for the GDH integral of ^3He below pion threshold is $\sim 140 \mu\text{b}$ [8]. This part equals the sum of the contributions from the three-body $\sim 170 \mu\text{b}$ ($\sim 130 \mu\text{b}$) and the two-body $\sim -30 \mu\text{b}$ ($\sim 10 \mu\text{b}$) components based on the calculations of Ref. [19] (Ref. [20]).

2. The experiment

The first experiment [7,8] on the three-body photodisintegration of ^3He using a longitudinally polarized ^3He target and a circularly polarized γ -ray beam took place at the HI γ S facility [25] of TUNL at the incident photon energies of 12.8 and 14.7 MeV. The AGS calculations [19] including single-baryon and meson-exchange electromagnetic currents (MEC), relativistic single-nucleon charge corrections (RC) [19] and the proton–proton Coulomb force using the method of screening and renormalization [19], provided a good description of the results.

To investigate further whether such an agreement continues as one goes to higher energy and resolve the discrepancy pointed out in Ref. [7] between the past unpolarized measurements, a new measurement of $^3\text{He}(\vec{\gamma}, n)pp$ was performed at the incident photon energy of 16.5 MeV and it is reported in this Letter. As in the previous experiment [7,8], a nearly mono-energetic, $\sim 100\%$ circularly-polarized pulsed γ -ray beam was used. The beam was collimated using a 12 mm diameter collimator resulting in on-target intensities of $(7.3\text{--}9.5) \times 10^7 \gamma/\text{s}$ and an energy spread of $\Delta\nu/\nu \leq 5.0\%$. A 10.6 cm long C_6D_6 cell was placed in the beam downstream of the target and two BC501A liquid scintillator neutron detectors were mounted at a scattering angle of 90° to detect the neutrons from deuteron photodisintegration. The on-target intensity of the beam was determined using the well-known $d(\gamma, n)p$ cross section [26].

Upstream of the flux monitor, the polarized γ -beam was incident on a polarized ^3He cell. The ^3He cell and the N_2 reference cell used for background subtraction were the same as in the previous experiment [7,8]. Details concerning their technical characteristics and the spin exchange optical pumping of the alkali metals used to polarize the ^3He target can be found in Refs. [7,8,

27–29]. The spin of the ^3He target was flipped every 15 min in order to extract the spin-dependent cross sections and the GDH integrand, $(\sigma^P - \sigma^A)/\nu$. The polarization was measured using the nuclear magnetic resonance-adiabatic fast passage [30] technique calibrated by electron paramagnetic resonance [31]. The latter can measure the absolute ^3He target polarization, P_t which was found to be between 33% and 37%.

An array of sixteen liquid scintillator BC-501A counters was used to detect only the neutrons from the $^3\text{He}(\vec{\gamma}, n)pp$ reaction since the kinetic energy of protons was not enough to straggle through the ~ 1 mm thick wall of ^3He cell. The detectors were placed in the horizontal plane every 15° , 1 m away from the center of the detector array, symmetrically on each side of the beam, at laboratory angles from 30° to 165° except for 60° and 120° due to the proximity to a pair of Helmholtz coils which provided the holding field for the polarized ^3He target.

3. Data analysis

Three quantities were recorded for each event: the pulse height (PH) of the neutron detector in ADC channels, the pulse shape discrimination (PSD) signal [32] and the time-of-flight (TOF) from the target to the detector in TDC channels.

The TOF measurements were carried out by measuring time intervals between events correlated with the γ -ray beam which is pulsed at a rate of 5.5 MHz (179 ns) [25]. A beam pickoff monitor (BPM) provides a signal coinciding with each beam pulse. The time difference between the BPM signal and each detected neutron provided the TOF and the energy of each event. The TDC channels were calibrated to TOF using a D_2O target. The zero point of the TDC was found using spectra acquired from the detection of the γ -rays scattered from an aluminum rod positioned at the center of the detector array. Extensive details about this technique and the electronics setup can be found in Refs. [7,33,34].

Initially, a PH cut was applied at $0.162 \text{ MeV} e_e^3$ to set the detector efficiency. The correlations between the PSD, PH and TOF were utilized and two-dimensional cuts were applied on these histograms to extract the neutrons and remove the γ -ray events. The same cuts were used for the data taken with the N_2 reference cell to subtract the background contributions. The outgoing neutron energy was determined using the measured TOF of the neutrons assuming they were emitted from the center of the ^3He target cell. The neutron detection efficiency varied rapidly as a function of neutron energy below 2.0 MeV. Therefore, we report cross sections only for neutrons with kinetic energies above 2.0 MeV. More details about this analysis can be found in Refs. [7,8].

The measured neutron background-subtracted yields (^3He neutron events/ N_γ) at the i th energy bin for target spin parallel/antiparallel to the helicity of the beam were calculated as $Y_{i,m}^{P/A} = Y_i^{P/A, ^3\text{He}} - Y_i^{N_2}$, where $Y_i^{P/A, ^3\text{He}}$ and $Y_i^{N_2}$ were the yields of reactions on ^3He and N_2 cells. Their linear combination led to the yields for parallel and antiparallel spin-helicity states $Y_i^{P/A} = \frac{1}{2}(Y_{i,m}^P(1 \pm \frac{1}{P_t P_b}) + Y_{i,m}^A(1 \mp \frac{1}{P_t P_b}))$, where P_b is the beam polarization. The double-differential cross sections were defined as

$$\frac{d^2\sigma^{P/A}}{d\Omega dE_n} = \frac{Y_i^{P/A}}{\Delta\Omega \Delta E \varepsilon_i N_t}, \quad (2)$$

where E_n is the neutron energy, $\Delta\Omega$ is the solid angle from the target to the neutron detector, ΔE is the width of the neutron energy bin, ε_i is the efficiency of the neutron detector calculated at

³ One MeV electron equivalent, $\text{MeV} e_e^3$, is the amount of light energy generated by an electron having kinetic energy of 1 MeV.

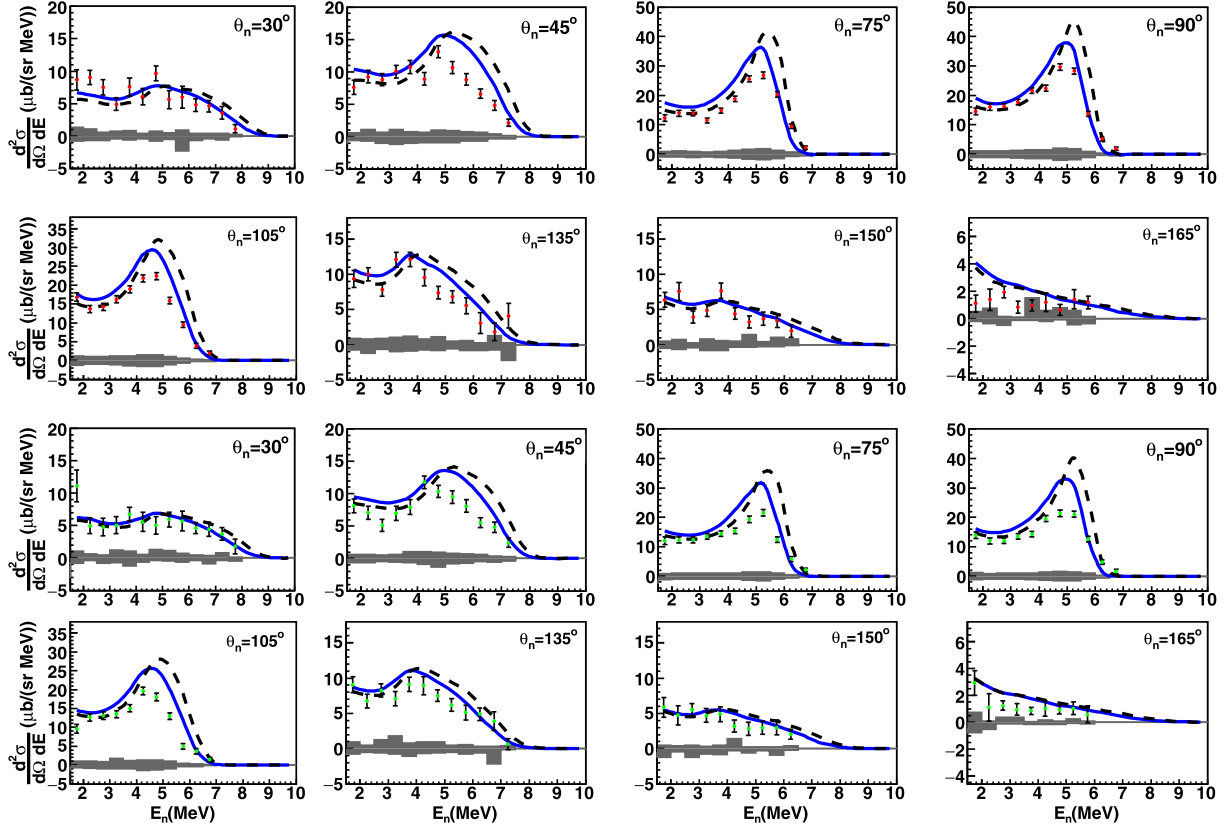


Fig. 1. (Color online.) Spin-dependent double-differential cross sections for the extended target for both parallel (two top rows) and antiparallel (two bottom rows) spin states for 8 neutron laboratory angles as a function of E_n , at $\nu = 16.5$ MeV. The solid-blue curve shows the GEANT4 simulation results based on the calculations of Ref. [19] including CD Bonn + Δ -isobar + RC + MEC + Coulomb force while the dashed-black curve is from Ref. [20] including AV18 + UIX + MEC. The neutron energy bin width is 0.5 MeV. The band shows the combined systematic uncertainties.

the i th energy bin using a GEANT4 [36] simulation of the experiment and N_t is the ^3He target thickness. The target thickness is defined as the product of the target length and its number density. The number density of the ^3He cell was measured using the broadening of the transition lines of the alkali metals due to the pressure of ^3He [35]. More details about this measurement can be found in Ref. [7]. N_t was determined to be $(8.3 \pm 0.3) \times 10^{21}$ atoms/cm 2 .

Two types of systematic uncertainties were identified: the bin-dependent and the overall normalization uncertainties. The former were asymmetric with respect to the centroid value of the cross section of each bin and arose from the PH cuts on the neutron spectra. The latter were bin-independent, symmetric and the major contributors from most to least important were: δP_b (5%), δP_t (4.2%), δN_γ (4.2%) (for which the main contribution was from the deuteron photodisintegration cross section uncertainty (3.0%) [26]), δN_t (4.0%), $\delta \varepsilon_i^{\text{sys}}$ (2.8%) [37,38] and $\delta \Delta\Omega$ (2%). The uncertainty of neutron energy E_n varied from 1% to 8% depending on the neutron laboratory angle and the outgoing neutron energy.

4. Results and discussion

The spin-dependent double-differential cross sections for the extended target obtained at an incident photon energy of 16.5 MeV for both spin-helicity states as a function of E_n are shown in Fig. 1. Instead of correcting the original data for the finite geometry effects [7], the theoretical calculations were convoluted with a GEANT4 simulation taking into account the finite target and the surrounding volumes. The solid and dashed curves are the GEANT4 simulation results using the calculations based on Ref. [19] and

Ref. [20], respectively. The band in each panel shows the overall systematic uncertainties combined in quadrature.

Although the magnitudes of the double-differential cross sections are overall larger in the parallel than those in the antiparallel spin-state, the distributions are not well described by either of these calculations. The bins close to the end-point energies of the laboratory scattering angles 30° (8.0–9.0 MeV), 45° (7.5–8.0 MeV), 150° (6.5–8.0 MeV) and 165° (6.0–8.0 MeV) were removed due to a relatively large background resulting in cross sections with large statistical uncertainties. The energy bins removed are given in the parentheses. Their contribution to the overall strength of the distributions was found to be $\sim 1\%$ for both spin-states and all scattering angles and it was added heuristically based on the theory.

Additional iterative Monte Carlo simulations using GEANT4 were carried out in order to correct the spin-dependent double-differential cross section distributions for finite-geometry effects [7]. The resulting corrected distributions were integrated over the neutron energy to extract the single differential cross sections. The unmeasured part of the distributions for $E_n < 2$ MeV was added based on the theoretical distributions including the Coulomb interaction which were normalized to the magnitude of the first valid neutron bin (2.0–2.5 MeV) for both states and all angles. Legendre polynomials up to the 4th order were used to fit the single differential cross section angular distributions for both states. To achieve the fit with the highest statistical significance, the single differential cross section points corresponding to the angle of 105° were removed. The $\chi^2/(\text{degrees of freedom})$ for the fit at the parallel (anti-parallel) state was found to be 1.01 (1.39). The fitting curves were integrated over the angle to extract the

Table 1

Total cross sections, σ^P and σ^A and the GDH integrand, $(\sigma^P - \sigma^A)/\nu$, with statistical uncertainties followed by systematics, compared with theoretical predictions.

	σ^P (μb)	σ^A (μb)	$(\sigma^P - \sigma^A)/\nu$ (fm^3)
This work	933 (12)(100)	764 (12)(91)	0.201 (21)(16)
Ref. [19]	1077	935	0.169
Ref. [20]	1099	979	0.143

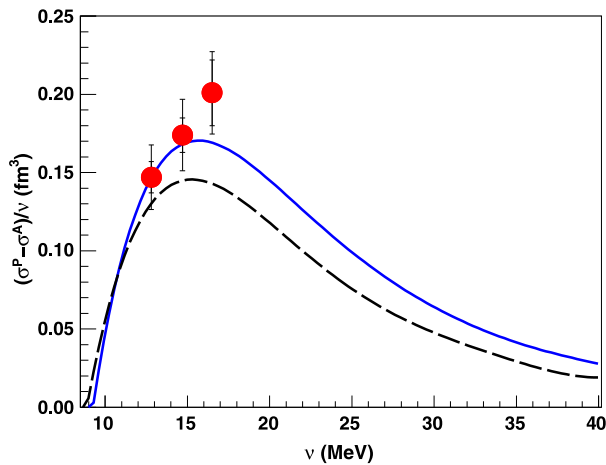


Fig. 2. (Color online.) The GDH integrand results (Ref. [7] and this work) compared with the theoretical predictions of Ref. [19] (solid-blue curve) and Ref. [20] (dashed-black curve). The inner error bars of the data points represent the statistical uncertainties while the outer include both the statistical and systematic uncertainties added in quadrature.

spin-dependent total cross sections and the value of the GDH integrand. More details about this analysis can be found in Refs. [7,8].

Table 1 summarizes the spin-dependent total cross sections and the contribution from the three-body photodisintegration to the ^3He GDH integrand together with the predictions based on the models presented in Ref. [19] and Ref. [20]. Differences between the measured spin-dependent total cross sections and the calculated values are found at the incident photon energy of 16.5 MeV. This is in contrast to the very good agreement observed between the previous measurements [7,8] and the calculations based on Ref. [19] at 12.8 and 14.7 MeV. The measured GDH integrand at 16.5 MeV was found to be slightly more than one standard deviation larger than the maximum calculated value based on Ref. [19]. Fig. 2 shows the contributions of the three-body photodisintegration of ^3He to the GDH integrand together with the theoretical predictions based on Refs. [19,20] as a function of the incident photon energy. To investigate whether the larger than expected GDH integrand value at 16.5 MeV is due to statistics, future measurements at higher energies are needed.

The unpolarized cross section was extracted as the average of the spin-dependent cross sections and was found to be equal to $(849 \pm 9 \pm 100) \mu\text{b}$. Fig. 3 shows all unpolarized total cross section data up to 30 MeV compared to the total cross section calculations from Ref. [19] (solid curve) and Ref. [20] (dashed curve). A general agreement between the two calculations and the experimental data can be observed for incident photon energy below 15 MeV. A serious discrepancy can be seen between different sets of data above 15 MeV while our result agrees with the measurements of Ref. [41] and the most recent data of Ref. [44] which favor smaller total cross section values above 15 MeV. In order to resolve the discrepancy among the unpolarized data and to further quantify the three-body contribution to the GDH integral, measurements above 16.5 MeV for this channel are necessary. These measurements combined with the recently acquired data from

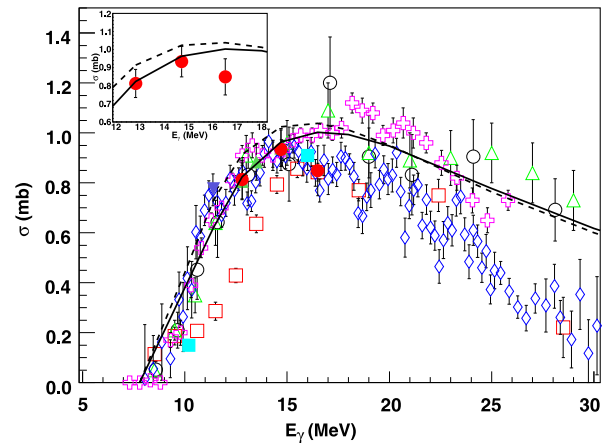


Fig. 3. (Color online.) All currently available total cross section data for the $^3\text{He}(\gamma, n)pp$ reaction up to 30 MeV: Ref. [7] and datum at 16.5 MeV presented for first time in this letter (filled circles), Ref. [39] (open circles), Ref. [40] (open squares), Ref. [41] (diamonds), Ref. [42] (open upward triangles), Ref. [43] (open crosses), Ref. [44] (filled squares), Ref. [33] (filled upward triangles), Ref. [45] (filled downward triangle) in comparison to the calculations from Ref. [19] (solid curve) and Ref. [20] (dashed curve). In the insert, the data by our collaboration are shown and compared with the theories. The older measurements [39–41,43] are presented with the statistical uncertainties while the newer data points [7,44,33,45] include both the statistical and systematic errors added in quadrature.

the two-body photodisintegration channel [8] will constrain the contribution to the GDH integral for ^3He below the pion threshold.

Acknowledgements

This work is supported by the U.S. DOE under contract numbers DE-FG02-03ER41-231, DE-FG02-03ER41-033, DE-FG02-03ER41-041, Duke University and the PNSC under Grant DEC-2013/10/M/ST2/00420. The numerical calculations of the Kraków group were performed on the clusters of the JSC.

References

- [1] S.D. Drell, A.C. Hearn, *Phys. Rev. Lett.* **16** (1966) 908; S.B. Gerasimov, *Yad. Fiz.* **2** (1965) 598, *Sov. J. Nucl. Phys.* **1** (1966) 430.
- [2] H. Dutz, et al., *Phys. Rev. Lett.* **93** (2004) 032003, and references therein.
- [3] H. Dutz, et al., *Phys. Rev. Lett.* **94** (2005) 162001, and references therein.
- [4] K. Slifer, et al., *Phys. Rev. Lett.* **101** (2008) 022303.
- [5] M.W. Ahmed, M.A. Blackston, B.A. Perdue, W. Tornow, H.R. Weller, B. Norum, B. Sawatzky, R.M. Prior, M.C. Spraker, *Phys. Rev. C* **77** (2008) 044005.
- [6] J. Ahrens, et al., *Phys. Lett. B* **672** (2009) 328, and references therein.
- [7] G. Laskaris, et al., *Phys. Rev. Lett.* **110** (2013) 202501; G. Laskaris, et al., *Phys. Rev. C* **89** (2014) 024002.
- [8] G. Laskaris, Ph.D. thesis, Duke University, 2015.
- [9] P. Aguar Bartolomé, et al., *Phys. Lett. B* **723** (2013) 71.
- [10] S. Costanza, et al., *Eur. Phys. J. A* **50** (2014) 173.
- [11] H. Gao, W. Chen, X. Zong, *Proc. Sci. CD09* (2009) 101.
- [12] H. Gao, et al., *Phys. Rev. C* **50** (1994) R546.
- [13] W. Xu, et al., *Phys. Rev. Lett.* **85** (2000) 2900.
- [14] S. Riordan, et al., *Phys. Rev. Lett.* **105** (2010) 262302.
- [15] X. Zheng, et al., *Phys. Rev. Lett.* **92** (2004) 012004.
- [16] X. Qian, et al., *Phys. Rev. Lett.* **107** (2011) 072003.
- [17] L.D. Faddeev, *Zh. Eksp. Teor. Fiz.* **39** (1960) 1459; L.D. Faddeev, *Sov. Phys. JETP* **12** (1961) 1041.
- [18] E.O. Alt, P. Grassberger, W. Sandhas, *Nucl. Phys. B* **2** (1967) 167.
- [19] A. Deltuva, L.P. Yuan, J. Adam, A.C. Fonseca, P.U. Sauer, *Phys. Rev. C* **69** (2004) 034004; A. Deltuva, A.C. Fonseca, P.U. Sauer, *Phys. Rev. C* **72** (2005) 054004; A. Deltuva, A.C. Fonseca, P.U. Sauer, *Annu. Rev. Nucl. Part. Sci.* **58** (2008) 27; A. Deltuva, A.C. Fonseca, P.U. Sauer, *Phys. Rev. C* **80** (2009) 064004.
- [20] R. Skibiński, J. Golak, H. Witała, W. Glöckle, A. Nogga, H. Kamada, *Phys. Rev. C* **72** (2005) 044002; R. Skibiński, J. Golak, H. Witała, W. Glöckle, H. Kamada, A. Nogga, *Phys. Rev. C* **67** (2003) 054002;

- R. Skibiński, J. Golak, H. Kamada, H. Witała, W. Glöckle, A. Nogga, Phys. Rev. C 67 (2003) 054001.
- [21] R.B. Wiringa, V.G.J. Stoks, R. Schiavilla, Phys. Rev. C 51 (1995) 38.
- [22] R. Machleidt, K. Holinde, Ch. Elster, Phys. Rep. 149 (1987) 1.
- [23] R. Machleidt, Phys. Rev. C 63 (2001) 024001.
- [24] J. Carlson, V.R. Pandharipande, R.B. Wiringa, Nucl. Phys. A 401 (1983) 59.
- [25] H.R. Weller, M.W. Ahmed, H. Gao, W. Tornow, Y.K. Wu, M. Gai, R. Miskimen, Prog. Part. Nucl. Phys. 62 (2008) 257.
- [26] D.M. Skopik, Y.M. Shin, M.C. Phenneger, J.J. Murphy II, Phys. Rev. C 9 (1974) 531;
Y. Birenbaum, S. Kahane, R. Moreh, Phys. Rev. C 32 (1985) 1825;
R. Bernabei, et al., Phys. Rev. Lett. 57 (1986) 1542;
A. De Graeve, et al., Phys. Rev. C 45 (1992) 860.
- [27] W. Happer, Rev. Mod. Phys. 42 (1972) 169.
- [28] K. Kramer, X. Zong, R. Lu, D. Dutta, H. Gao, X. Qian, Q. Ye, X. Zhu, T. Averett, S. Fuchs, Nucl. Instrum. Methods Phys. Res., Sect. A 582 (2007) 318.
- [29] Q. Ye, G. Laskaris, W. Chen, H. Gao, W. Zheng, X. Zong, T. Averett, G.D. Cates, W.A. Tobias, Eur. Phys. J. A 44 (2010) 55.
- [30] W. Lorenzon, T.R. Gentile, H. Gao, R.D. McKeown, Phys. Rev. A 47 (1993) 468.
- [31] M.V. Romalis, G.D. Cates, Phys. Rev. A 58 (1998) 3004, and the references therein.
- [32] Mesytec GmbH & Co. KG, Four channel particle discriminator module for liquid scintillators, <http://www.mesytec.com/datasheets/MPD-4.pdf>.
- [33] B.A. Perdue, Ph.D. thesis, Duke University, 2010;
B.A. Perdue, M.W. Ahmed, S.S. Henshaw, P.-N. Seo, S. Stave, H.R. Weller, P.P. Martel, A. Teymurazyan, Phys. Rev. C 83 (2011) 034003.
- [34] J.M. Mueller, Ph.D. thesis, Duke University, 2013.
- [35] K.A. Kluttz, T.D. Averett, B.A. Wolin, Phys. Rev. A 87 (2013) 032516;
K.A. Kluttz, Ph.D. thesis, The College of William and Mary, 2012.
- [36] S. Agostinelli, et al., Nucl. Instrum. Methods Phys. Res., Sect. A, Accel. Spectrom. Detect. Assoc. Equip. 506 (2003) 250.
- [37] D.E. González Trotter, F. Salinas Meneses, W. Tornow, A.S. Crowell, C.R. Howell, D. Schmidt, R.L. Walter, Nucl. Instrum. Methods Phys. Res., Sect. A, Accel. Spectrom. Detect. Assoc. Equip. 599 (2009) 234.
- [38] H.R. Setze, et al., Phys. Lett. B 388 (1996) 229.
- [39] A.N. Gorbunov, A.T. Varfolomeev, Phys. Lett. 11 (1964) 137.
- [40] H.M. Gerstenberg, J.S. O'Connell, Phys. Rev. 144 (1966) 834.
- [41] B.L. Berman, S.C. Fultz, P.F. Yergi, Phys. Rev. C 10 (1974) 2221.
- [42] A.N. Gorbunov, in: D.V. Skobel'tsyn (Ed.), Photonuclear and Photomesic Processes, vol. 71, Consultants Bureau, New York, 1974, pp. 1–117.
- [43] D.D. Faul, B.L. Berman, P. Meyer, D.L. Olson, Phys. Rev. C 24 (1981) 849.
- [44] S. Naito, et al., Phys. Rev. C 73 (2006) 034003.
- [45] X. Zong, Ph.D. thesis, Duke University, 2010.